Journal of Hydrology 580 (2020) 124199

Contents lists available at ScienceDirect

Journal of Hydrology

journal homepage: www.elsevier.com/locate/jhydrol

Research papers

Physical modeling investigation of rainfall infiltration in steep layered volcanoclastic slopes

Giovanna Capparelli[a,*], E. Damiano[b], R. Greco[b], L. Olivares[b], G. Spolverino[a]

[a] Dipartimento di Ingegneria Informatica, Modellistica, Elettronica e Sistemistica, Università della Calabria, Italy
[b] Dipartimento di Ingegneria, Università degli Studi della Campania "L. Vanvitelli", Italy

ARTICLE INFO

This manuscript was handled by Corrado Corradini, Editor-in-Chief, with the assistance of Philip Brunner, Associate Editor

Keywords:
Infiltration processes
Physical flume model
Layered pyroclastic deposits

ABSTRACT

Infiltration processes in layered slopes can be strongly affected by the different hydraulic properties of the soils constituting the layers, with potential downslope flow diversion that can have effects on slope stability as well as on runoff generation and groundwater recharge. In this respect, volcanoclastic soil covers represent a typical example, as layers with strongly contrasting textures are deposited during the various eruptive phases. In this paper, the results of a transient infiltration test, carried out in a densely instrumented physical model of a layered volcanoclastic sloping cover, are presented. The soil cover was constituted by a layer of gravelly pumices interbedded between two layers of finer ashes (sandy loams). Even with such an extreme contrast in texture, capable of significantly delaying the advancement of infiltration through the layer of pumices, flow diversion occurred only temporarily at the interface between the upper layer of ashes and the pumices. In fact, although a long-lasting intense rainfall was applied into an initially dry soil profile, the downslope diverted water volume in form of a subsurface runoff was just a small fraction of the total applied rainfall. In fact, the accumulation of water above the upper edge of the pumices, responsible of the subsurface runoff, soon led to the establishment of a large water potential gradient, which redirected the infiltrating flow through the pumices and stopped the downslope flow diversion.

1. Introduction

Granular shallow covers involved in rainfall-induced landslides are spread throughout the world. In the case of slopes covered by cohesionless deposits and characterized by inclination larger than the friction angle of the soils, the slope stability is guaranteed by the contribution to soil shear strength offered by matric suction in unsaturated conditions (e.g. Fredlund and Morgenstern, 1977; Vanapalli et al., 1996; Wheeler et al., 2003; Lu et al., 2010; Greco and Gargano, 2015). During rainwater infiltration, increase of soil moisture, causing the reduction or even the vanishing of suction, can lead to landslide triggering (e.g. Collins and Znidarcic, 2004; Baum et al., 2010; Lu and Godt, 2008; Damiano and Olivares, 2010; Greco et al., 2013). Hence, the analysis of the water balance of the slope, accounting for infiltration, evapotranspiration and drainage, is mandatory for the assessment of slope instability conditions (Bogaard and Greco, 2016; Formetta et al., 2016). In the simple case of a slope with regular geometry, in presence of homogeneous and isotropic covers, the infiltration flow direction is orthogonal to ground surface when the capillary gradient dominates (i.e. in unsaturated conditions), while it becomes vertical when, approaching saturation, the flow tends to be gravity driven (e.g. Lu et al., 2011). When the infiltrating flow reaches the interface between soil cover and bedrock, depending on its hydraulic behavior drainage may occur either as leakage to recharge groundwater circulation (e.g. Jukić and Denić-Jukić, 2009; Soulsby et al., 2011; Allocca et al., 2015), or as subsurface runoff along the interface (e.g. Freer et al., 2002; Sidle et al., 2000; Tromp-van Meerveld and McDonnell, 2006; Lanni et al., 2013). In the case of heterogeneous and layered soil profiles the analysis of the infiltration process becomes more complex, as contrasting hydraulic properties of adjoining layers may induce locally diverted flow (e.g. Ross, 1990; Warrick et al., 1997; Yang et al., 2006; Schneider et al., 2014; Hübner et al., 2017; Formetta and Capparelli, 2019).

The influence of layers of coarse-grained soils has been studied and exploited for the case of artificial layered covers, such as those realized to prevent infiltration into landfills. In this case, layers of extremely contrasting texture are used, so to exploit the so-called phenomenon of the capillary barrier. In fact, in unsaturated conditions, coarse layers are characterized by small retention capacity and hydraulic conductivity, so to confine infiltrating water within the overlying layers

* Corresponding author.
E-mail address: giovanna.capparelli@unical.it (G. Capparelli).

https://doi.org/10.1016/j.jhydrol.2019.124199
Received 31 July 2019; Received in revised form 26 September 2019; Accepted 30 September 2019
Available online 11 October 2019

and divert downslope the flow. In this respect, several studies have been carried out to define the most effective sequence and textural composition of the layers (e.g. Khire et al. 2000; Aubertin et al. 2009; Rahardjo et al., 2013; Zhan et al., 2014).

Soil layering is often observed in natural slopes. In residual soil covers, where weathering of the soil profile is maximum at the ground surface, and vanishes with depth, until the parent material is found, the soil profile usually presents porosity gradually decreasing with depth, and the finest-textured layers at the top (e.g. Wallace, 1973; Rahardjo et al., 2004). In pyroclastic covers, the layering depends on the history of deposition of the materials spewed out by the eruptions and on the following weathering processes. As a result, pyroclastic soil profiles often present several layers with contrasting textural and physical characteristics.

In Campania (southern Italy), several eruptions of large volcanic complexes, i.e. Somma-Vesuvius, Phlegrean Fields and Roccamonfina, occurred during the last 40,000 years (Rolandi et al., 2003). The resulting materials are spread over a wide area around the city of Naples, and the slope covers are often interested by rainfall-induced landslides (e.g. Cascini et al., 2008a; Revellino et al., 2008; Di Martire et al., 2012). Depending on the distance from the eruptive center and on the direction of the wind blowing during the eruption, the air-fall deposition of the materials gave rise to soil covers with spatially variable characteristics, in terms of number, thickness and properties of the soil layers constituting the profile (Del Soldato et al., 2018; De Vita et al., 2006). Weathering processes occurred in between the eruptions also affect the physical properties of the various layers. The highest textural contrast is usually observed between adjoining layers constituted by pumices (gravels with sand) and ashes (loamy sands).

The volcaniclastic soils of Campania, often characterized by very high porosity (e.g. up to 0.7–0.75) and saturated hydraulic conductivity reaching 10^{-5}–10^{-4} m/s (Basile et al., 2003; Bilotta et al., 2005; Damiano et al., 2012; Sorbino and Nicotera, 2013; Vingiani et al., 2015), are cohesionless or exhibit very small cohesion, and normally remain unsaturated also during the rainiest periods (Cascini et al., 2014; Comegna et al., 2016; Napolitano et al., 2016).

As the soils usually exhibit null or very small cohesion (e.g. Bilotta et al., 2005; Sorbino and Nicotera, 2013; Olivares et al., 2019), and the air-fall deposited materials often rest along slopes with inclination close to the friction angle of the soils (e.g. De Vita et al., 2006), slope failure often occurs in saturated or nearly saturated conditions (e.g. Damiano and Olivares, 2010)

Several studies investigated how layering affects the infiltration process through the volcanoclastic covers of Campania and the eventual triggering of landslides (Cascini et al., 2008b; Damiano et al., 2017; Damiano and Olivares, 2010; Mancarella et al., 2012). Although some authors argued that in some cases the pumices may act as a capillary barrier, through which water can pass only if a critical value of the water potential is attained (Ross, 1990; Stormont and Anderson, 1999), the behavior of volcanoclastic layered profiles during infiltration is more complex, as it depends on initial moisture conditions and on the infiltration rate. In initially dry conditions, the deepening of the wetting front can be hindered by the coarse layers of pumices, characterized by small unsaturated hydraulic conductivity. Differently, in wet conditions, the finer ash layers present the smallest hydraulic conductivity and prevent the penetration of the wetting front.

In both cases, the accumulation of water within the soil profile may lead to the establishment of subsurface downslope flow, which, depending on the intensity and duration of rainfall, and on the morphology of the considered hillslope, can either enhance slope drainage, with positive effects on slope stability, or cause flow concentration leading to local failure (Damiano, 2018).

However, the effects of soil cover layering on drainage processes in natural slopes have not been investigated so far. In fact, most of the experimental studies, dealing with infiltration through layered slopes, focused on water potential and water content trends within the soil cover (Damiano et al. 2017; Capparelli and Versace, 2014; Formetta et al., 2016; De Vita et al., 2018), while little attention has been paid to the quantification of the diverted flows. Useful information for the quantitative prediction of the diverted flows can be provided by the analysis of transient infiltration experiments through layered sloping covers, either in the field (e.g. Tallon et al., 2011; Schneider et al., 2014; Hübner et al., 2017) or in physical models in laboratory (e.g. Walter et al., 2000; Kämpf et al., 2003; Tami et al., 2004; Olivares et al., 2009; Spolverino et al., 2019). Specifically, physical modeling allows getting rid of many factors affecting flow processes (e.g. vegetation, heterogeneity of soil properties, irregular layer geometry), focusing solely on the effect of the layers.

Aim of this study is to investigate the possible flow diversion in a deposit characterized by a layer of pumices, interbedded through layers of ashes. Indeed, flow diversion may affect slope stability as well as several hydrological processes occurring along the studied slopes, such as runoff generation, groundwater recharge. To this aim, the results of transient infiltration experiments, carried out in a physical model of a layered volcanoclastic slope, reconstituted in an instrumented experimental flume, are presented. It is equipped with a series of devices, which allow monitoring soil wetting during the entire experiment and the measurement of the outflow from the different layers at the foot of the slope, so to identify the conditions leading to the establishment of downslope flows.

2. Materials and methods

To study the behavior of layered volcanoclastic deposits during infiltration and drainage processes, an experimental campaign has been carried out in a small scale model of a layered slope. In the following subsections, the main physical properties of the soils used to reconstitute the deposit, the characteristics of the physical model, and the series of experiments are described.

2.1. Soil properties

Aiming at studying the effects of layers with contrasting textural and hydraulic properties on the dynamics of infiltration and drainage processes developing in sloping volcanoclastic deposits, two soils of markedly different characteristics have been used. The two soils have been collected along the slope of Pizzo d'Alvano, close to the village of Episcopio, near Sarno, a town 30 km from Naples (Italy), surrounded by mountains covered with layered pyroclastic deposits laying upon fractured carbonate bedrock (Fig. 1a). Along the slopes of these mountains, on 5th May 1998, a series of catastrophic debris flows were triggered by a rainstorm of about 120 mm in 48 h (Del Prete at al., 1998; Cascini, 2004; Cascini et al., 2008a,b).

Specifically, the two soils were collected along a slope with inclination angle of 20°, from horizons belonging to the soil profile originated by eruption of 1780–1800 B.C. of Somma-Vesuvius, designated as Bb and Cb in Fig. 1b.

The first soil (horizon Bb) is a volcanic ash with porosity ranging between 0.62 and 0.66. The second soil (horizon Cb) is constituted by pumices of the eruption of 1780–1800 B.C. Fig. 2 shows the grain size distribution of the two soils, determined by sieving according to the standard ISO 11277:2009. Specifically, the USDA soil classification of the ashes is sandy loam, with a grain size distribution already observed in other studies in Pizzo D'Alvano (e.g. Terribile et al., 2000; De Vita and Piscopo, 2002; Bilotta et al., 2005), while the pumices are a sandy gravel. Table 1 gives the main physical and mechanical properties of the two soils, as derived by experiments on small specimens (Olivares et al., 2019; Guadagno, 1991; Basile et al., 2003; De Vita et al., 2013) and mathematical model calibration (Capparelli and Versace, 2014).

It is worth to note that the two soils have been selected as they present two of the most contrasting textures of adjoining layers among the horizons usually found in the volcanoclastic layered deposits of

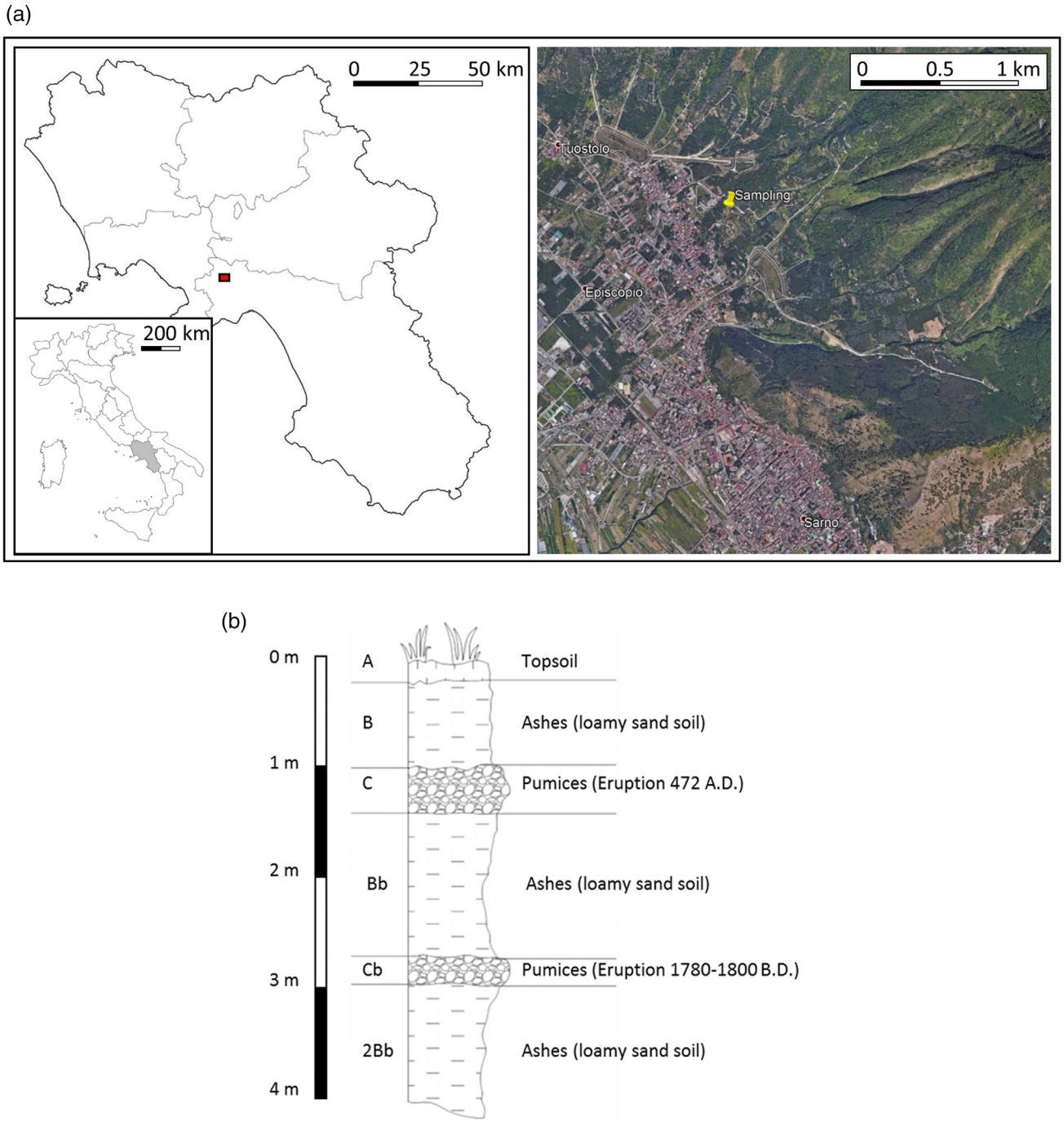

Fig. 1. Sketch of the layered soil profile in the site of soil sample collection (modified after Capparelli et al., 2018).

Campania. Consequently, it is expected that also their hydraulic behavior in unsaturated conditions should present quite different features, in terms of both water retention capacity and hydraulic conductivity. This should strongly affect infiltration and drainage processes developing in a layered deposit constituted by such soils.

2.2. Slope model

The physical model has been built in the experimental flume available at the Laboratory of Environmental Cartography and Hydrogeological Modeling (Camilab) of the Università della Calabria, which allows deeply analyzing the infiltration process in slopes with layered deposits with thickness close to that of real slopes, by measuring both overland and subsurface runoff. It consists of two connected independently tilting flume branches (respectively designed to study landslide triggering and propagation), each 1 m wide and 3 m long. The flume is equipped with tensiometers for measuring soil water potential inside the slope, Time Domain Reflectometry (TDR) system and probes for measuring soil volumetric water content, and laser transducers for measuring soil surface displacements in the direction orthogonal to the sliding plane. More details about the experimental flume can be found in Spolverino et al. (2019). The longitudinal section and plan view of the model are reported in Fig. 3.

The experimental flume is provided with two series of nozzles along both sides, connected to a digitally controlled pressurized water circuit, able to sprinkle an artificial rainfall of controlled intensity all over the

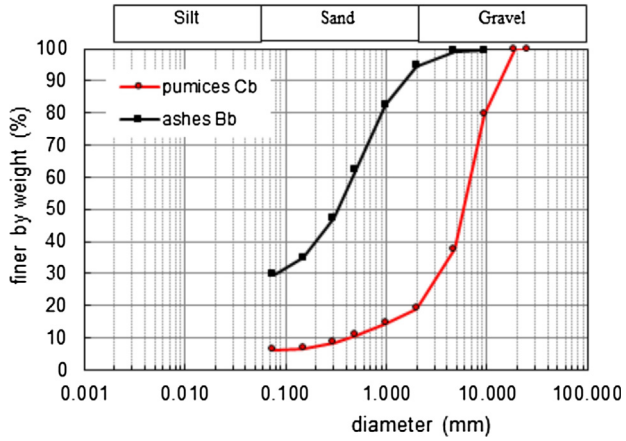

Fig. 2. Particle size distributions of the two soils used to build the layered deposit.

Table 1
Main physical properties of the investigated soils (G, specific gravity; n, porosity; k_{sat}, saturated hydraulic conductivity; c′, effective cohesion; ϕ′, friction angle). The values of the parameters have been taken from Olivares et al. (2019); Guadagno et al. (1999); Basile et al. (2003); De Vita et al. (2013).

Soil	G	N (%)	k_{sat} (m/s)	c′ (kPa)	ϕ′ (°)
Ashes	2.61	68	6.10^{-7}	0	37
Pumices	2.4–2.5	30–42	2.10^{-3}	0	38–45

model. To monitor the actual rainfall intensity applied to the slope, two tipping bucket rain gauges, located in two different positions within the flume, are also available.

The reconstituted layered deposit was 270 cm long and 60 cm wide, and it consisted of a 10 cm thick layer of pumices interbedded between two layers of ashes. Both the upper and lower layers of ashes had a thickness of 20 cm. The ratio between the thickness and the length of the model did not allow to consider the slope as infinite, although such a simplified geometry would be of help for the interpretation of the experimental results. However, the adopted boundary conditions, described hereinafter, were such that the flow in the deposit was mostly driven by potential energy gradients directed vertically or orthogonally to the slope surface (i.e. related to gravity and capillarity, respectively), thus limiting the extension of the zones affected by uphill and downhill boundaries. The layers were reconstituted in the flume with the moist tamping technique, following the procedure described in Olivares et al. (2009), so to obtain a packing of the soil particles which was similar as the one of natural covers in primary deposition conditions. Aiming at achieving a homogeneous and balanced water potential distribution before the infiltration experiment, the layered deposit, initially in horizontal position, was subjected to a series of wetting and equalization/evaporation phases, which lasted in total three months. Afterwards, the deposit was tilted to an inclination angle of 38°, and an equalization phase of two more weeks was carried out, so to attain a nearly hydrostatic distribution of water potential. The choice of the inclination angle of 38°, equal to the friction angle of the ashes (Table 1), was made to prevent the failure of the slope, during the infiltration test, before the attainment of complete saturation. During the wetting/drying cycles, the upper layer of ashes, initially very loose, experienced a volumetric strain in the order of 3%, which resulted in a mean reduction of the total thickness of the deposit of about 0.6 cm, which was detected by the laser transducers. Table 2 reports the characteristics of the layered deposit before the beginning of the infiltration test. Two pictures showing the physical model of the layered slope in the experimental flume are given in Fig. 4.

Aiming at detecting the effects of the layers on the infiltration process, the deposit was equipped with 10 tensiometers, located at four different depths, approximately along three alignments, orthogonal to the slope surface, near the center of the deposit, and 8 TDR probes located at three depths along the same alignments. The TDR probes, consisting of three parallel metallic rods 10 cm long and with an external interspace of 3 cm, were buried in the soil deposit with the rods parallel to the slope inclination. The tensiometers were the miniaturized type (Soil Moisture Inc.), characterized by ceramic cups 3 cm long and 1.5 cm wide, which were placed with their longer axis orthogonal to the slope. In this way, although the soil volumes sampled by the two different sensors were quite different (i.e. about 70 cm^3 for the TDR probes, about 10 cm^3 for the tensiometers), their dimension in the direction of the propagation of the wetting front were similar (i.e. about 3 cm in both cases). Hence, the different sampling volumes might affect the observed results especially whereas the infiltration process were not homogeneous.

While the TDR probes were buried in all the three layers, the tensiometers could not be placed within the layer of pumices, as their very coarse gravelly nature do not allow the establishment of the required hydraulic contact between the soil and the tensiometer cap. So, the tensiometers were placed close to the upper and lower interfaces between pumices and ashes. In Fig. 5, the sketch of the longitudinal section of the deposit is shown, with the indication of the position of tensiometers and TDR probes.

To increase the reliability of soil volumetric water content estimates provided by TDR, the interpretation of the measurements was carried out with a soil-specific calibration curve, experimentally determined over reconstituted samples of the ashes (Capparelli et al., 2018).

The deposit was confined at all the sides by plexiglass panels, so to have impervious boundaries. The only exception was the flume cross section at the foot of the slope, where a seepage face boundary condition was realized, by means of a perforated metal panel, with circular holes with diameter of 0.5 cm, regularly spaced every 0.7 cm. Interbedded between the soil deposit and the panel, a layer of geotextile was placed, so to prevent the detachment of soil particles. The perforated panel, shown in Fig. 6, was provided with gutters at the base of each soil layer, as well as in correspondence of the top soil surface, so to separately collect, at the foot of the slope, water outflow from the three layers and overland runoff. The measurement of the outflow rates was carried out with tipping bucket rain gauges located at the outlet of each.

2.3. Infiltration test

Aim of the infiltration test was the assessment of the establishment of downslope flow components caused by the adjoining layers with different textural and hydraulic characteristics, paying specific attention to the interface between the upper layer of ashes and the pumices, where a capillary barrier effect could arise.

According to the research objectives, experimental conditions were determined with the aim of emphasizing the conditions, which could promote the phenomenon. Therefore, both the applied rainfall intensity, its duration and the succession of the various phases have been defined based on the observed results. Summarizing, the main steps that have been carried out were:

I. Initially a high rainfall intensity (i.e. about 32 mm/h) was applied.
II. After about 20 min, an intense overland runoff was activated, thus subtracting part of the rainfall from the infiltration process.
III. The rainfall intensity was reduced to about 9 mm/h, constant until the wetting front reached the base of the upper layer of ashes.
IV. After about 2.5 h from the beginning of the test, rainfall intensity was increased to about 50 mm/h, and it was interrupted when a large part of the upper layer of ashes started sliding, leaving some of the sensors uncovered.

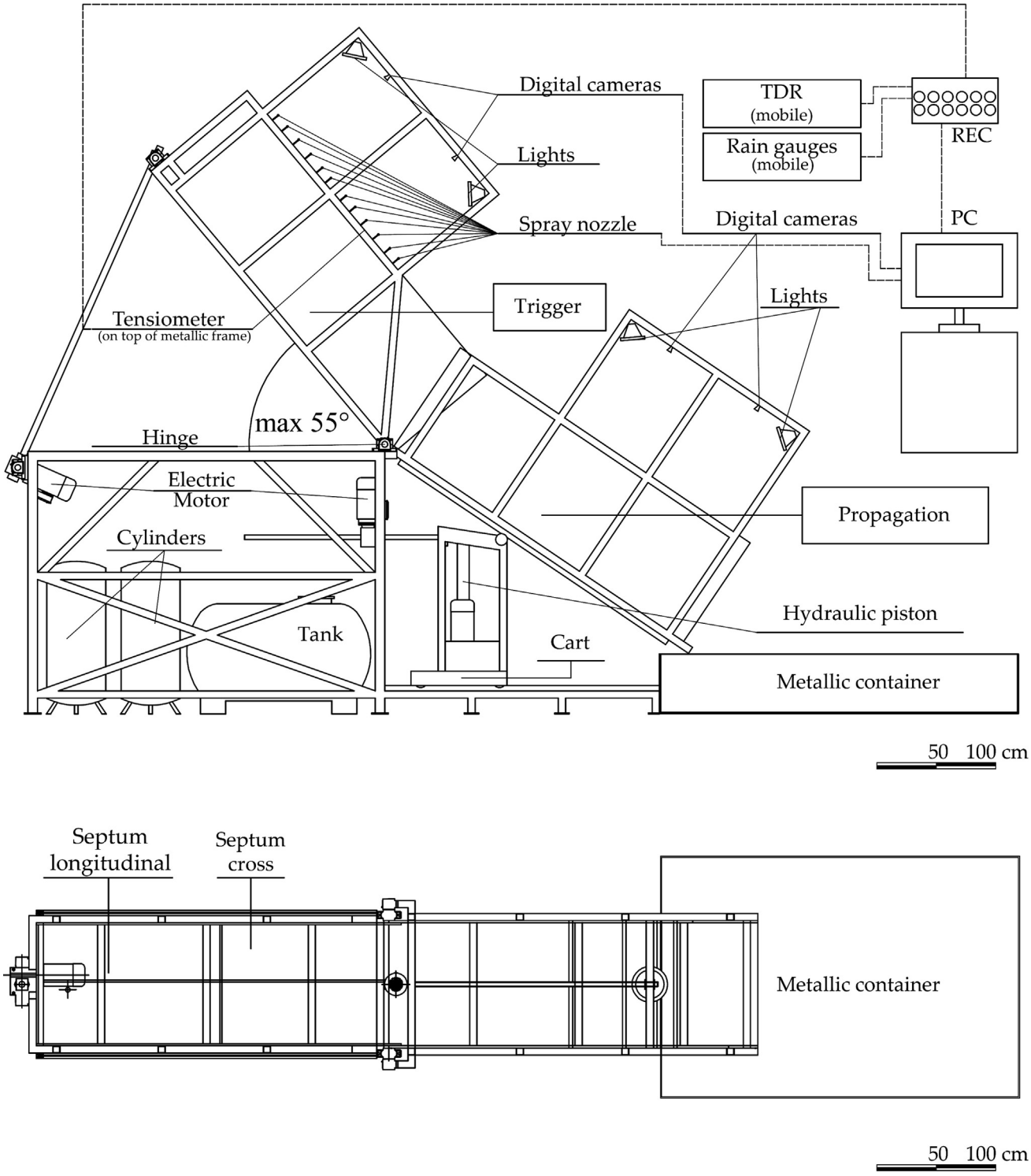

Fig. 3. Longitudinal section and plan view of the mechanical components of the experimental flume (modified after Spolverino et al., 2019).

The total duration of the infiltration was 257 min, with a mean rainfall intensity of 27.5 mm/h, corresponding to a return period of about 100 years, according to the depth duration frequency curves of extreme rainfall of the area of Pizzo d'Alvano. Afterwards, some of the sensors kept acquiring data until 350 min. Table 3 summarizes the details of the various phases of the test.

3. Results and discussion

Fig. 7 shows the trend of pore water pressure as measured by the tensiometers installed at various depths and positions within the layered deposit. The upper three tensiometers, placed within the uppermost layer of ashes at the depth of 6.5 cm below the soil surface (i.e. tensiometers T2, T4 and T9 of Fig. 7), responded nearly simultaneously and showing quite similar increasing trends of pressure. This indicates that the applied rainfall intensity could be considered homogeneous

Table 2
Main characteristics of the layers of the physical model at the beginning of the test.

Soil	Tickness	Porosity	Initial volumetric water content	Initial suction	
	(cm)	(%)	(%)	depth (cm)	(kPa)
Upper ashes	19.4 (initially 20 cm, reduced after volumetric strain in the test preparation phase)	58–63 (initially 62–66, reduced after volumetric strain in the test preparation phase)	22–26	6	46–49
				18.5	43–47
Pumices	10	not available	5–8	–	
Lower ashes	20	62–66	18–23	32	36–38
				48.5	27–28

throughout the entire physical model. Differently, the three tensiometers buried at the depth of 18.5 cm within the same layer (i.e. tensiometers T1, T3 and T10 in Fig. 7) clearly indicate that the progress of the infiltration followed quite a delayed and smoother trend in the upslope alignment, compared to both the other two, which still resulted very similar to each other, with the middle alignment responding slightly before the downslope one. Such a slower infiltration in the upper part of the model should be likely ascribed to some possible influence of the upper impervious boundary, although 1 m far, and to some local soil heterogeneity, as also confirmed by the time history of soil water content, reported in Fig. 8 as measured by the TDR probes. In fact, probe S6 showed a much slower soil wetting, compared to probe S8 and, even more, to probe S7. The response of the TDR probes at the depth of 18.5 cm was generally delayed with respect to the tensiometers placed in close positions, with the water content that started changing only when the corresponding tensiometer registered pore pressure above −15 kPa (the response delay was between 30 and 35 min for the various probes). This was probably due to the combined effect of the non-linearity of soil water retention curve (i.e. coarse-grained ashes showing quite a small water content variation in the pressure range between −50 kPa and −15 kPa), and of the response of the TDR probes, which are sensitive to the spatial average of the water present within the investigated soil volume (e.g. Zegelin et al., 1989), compared to the tensiometers, quickly responding to water coming in contact with the porous caps.

Regardless of the heterogeneous response along the three investigated alignments, in all cases a strong water potential gradient developed across the upper ashes during the first 40–90 min (depending on the alignment). This indicates that, in this phase, the infiltration flow was essentially orthogonal to the slope. Afterwards, all the tensiometers placed in the upper layer reached quite similar pressure values, namely around −3.0 kPa. In these conditions, the water flow tended to be driven by the unit gravitational potential gradient, thus becoming essentially vertical. The vertical infiltration rate was therefore close to the unsaturated hydraulic conductivity of the soil, which can therefore be estimated around 9 mm/h.

As often observed when large scale experiments are carried out and thus soil structural porosity is involved in the flow near saturation, the hydraulic conductivity results much higher than what is estimated on small specimens, as reported in Table 1. However, both the water content and the estimated hydraulic conductivity at −3.0 kPa seem in line with the unsaturated behavior of the soil B from Pizzo D'Alvano described by Bilotta et al. (2005), presenting physical characteristics resembling those of the ashes tested here.

Fig. 8 shows that the TDR probes placed in the layer of pumices started registering an increase of soil water content at quite different times, and in the same order as in the overlying layer of ashes. Specifically, wetting was registered first in the middle alignment, after about 140 min. About 10 min later, the wetting front in the pumices was detected in the downslope section. Finally, in the upslope alignment, a steep wetting front arrived after about 200 min from the beginning of the test.

This indicates that the building of the water pressure gradient, needed for the water to penetrate the dry pumices, was controlled by

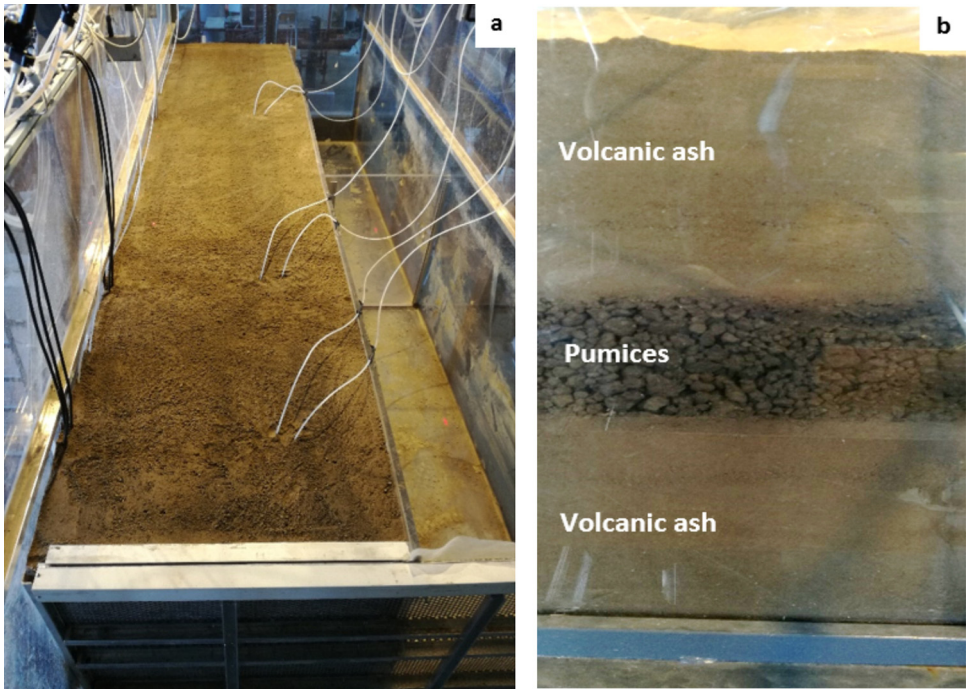

Fig. 4. Physical model of the layered slope in the experimental flume: top view (a) and detail of the layered deposit (b).

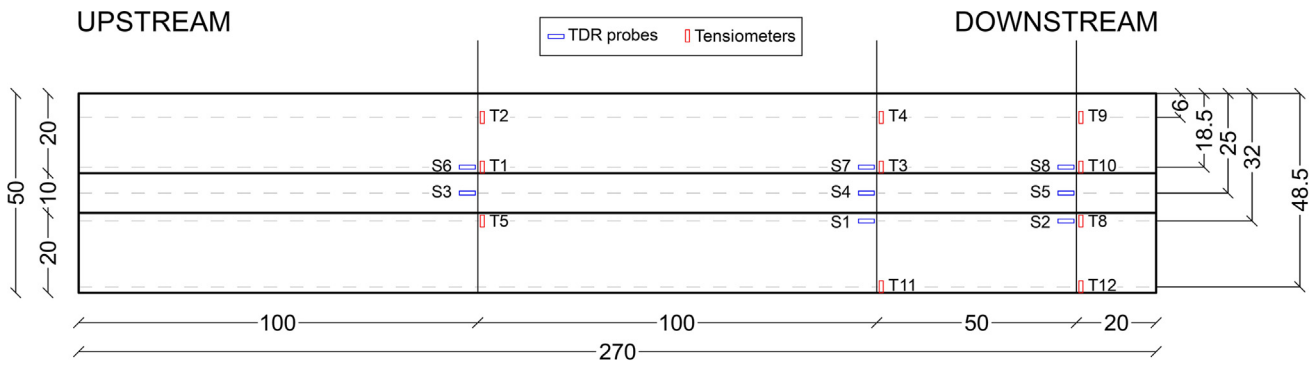

Fig. 5. Sketch of the longitudinal section of the physical model of a layered slope, with the indication of installed tensiometers (indicated with T) and TDR probes (indicated with S).

Fig. 6. View of the perforated panel, placed at the foot of the physical model of a layered slope, aimed at realizing a seepage face boundary condition, and provided with gutters (indicated with the red arrows) for the separate collection and measurement of overland and subsurface runoff coming from the three layers. (For interpretation of the references to colour in this figure legend, the reader is referred to the web version of this article.)

Table 3
Main phases of the infiltration experiment carried out in the physical model of a layered slope.

Steps	Time from the beginning of the test (min)	Rainfall intensity (mm/h)
I	0–18	32
II	18–151	9
III	151–257	50
IV	257-onward	0

the wetting of the uppermost layer of ashes.

As it can be seen in Fig. 7, in both the upslope and downslope alignments, the water reached the middle of the pumices about 50 min after the establishment of the maximum water potential gradient across the layer of pumices, i.e. when the tensiometer at the depth of 18.5 cm had reached the value of −3.0 kPa, while the tensiometer below the pumices (at the depth of 32 cm) was still recording the initial water pressure around 38–40 kPa (after about 90 min for the downslope alignment, and after 150 min upslope).

Considering that initially the pumices were at a pressure between −40 kPa and −50 kPa, as indicated by the initial values of the tensiometers T1, T3, T5, T8 and T10 in Fig. 7, this result indicates that a water potential gradient of several meters over few centimeters had to develop to let water enter the pumices. This implies that, in these conditions, the unsaturated hydraulic conductivity of the pumices was more than two orders of magnitude smaller than the adjoining ashes, i.e. in the order of 10^{-8} m/s.

The time, needed for the building up of such a high gradient, caused a delay in the progress of infiltration and an accumulation of water within the upper layer of ashes (Figs. 7 and 8).

This delay is even more evident in the graphs of Fig. 9. Specifically, Fig. 9a reports the time at which the tensiometers installed at the various depths recorded the arrival of the wetting front. Similarly, in Fig. 9b, the arrival times of the wetting front as detected by TDR probes, installed also within the layer of pumices, are reported.

The inclination of the lines plotted in the graphs of Fig. 9 gives an estimate of the propagation speed of the infiltration process (i.e. the more inclined the line is, the faster was the phenomenon), clearly showing that the phenomenon progressed more slowly through the pumices than in the ashes. It is worth to note the substantial agreement between the wetting front propagation speed estimated by TDR probes and tensiometers. In fact, the slight delay of soil moisture increment, compared to that of suction, can be ascribed not only to the different sampling volumes of the two sensors, but mainly to the strong non-linearity of the wet branch of the soil water retention curve.

Nonetheless, the outflow from the upper layer of ashes, measured at the perforated panel placed in the downslope section of the flume and plotted in Fig. 10, did not seem to indicate the establishment of a significant subsurface runoff through the upper layer of ashes. In fact, only between 40 and 50 min from the beginning of the test a peak of about 6.5 l/h was observed. Afterwards, the outflow first reduced to about 0.6 l/h, and then increased again to about 2 l/h after 130–140 min (Fig. 10).

The discharge of 6.5 l/h outflowing from the upper layer of ashes indicates the temporary establishment of a significant downslope-directed subsurface runoff. In fact, even considering the high rainfall intensity of 32 mm/h initially applied, the outflow corresponding to a vertical flow through such a layer would only correspond to about 2.3 l/h (considering the projection over a horizontal plane of the inclined outflow section, as sketched in Fig. 11a). The observed flow rate, likely outflowing through only the lowest part of the upper layer cross section (see Fig. 11b), corresponds to such a high specific discharge (i.e. of the order of 100 mm/h), that it can be argued that, between 40 and 50 min from the beginning of the test, a saturated (or nearly saturated) layer formed in the ashes at the foot of the slope, near the interface with the underlying pumices.

Differently, the discharge of about 0.6 l/h observed between 50 and 120 min exactly equals the outflow caused by a vertical infiltration at a rate of 9 mm/h, thus confirming the establishment of vertical flow already argued from the tensiometer readings. The value of nearly 2 l/h observed from 140 to 170 min, and then slowly decreasing, despite the strong increase of the applied rainfall, also does not seem to indicate the persistence of a significant downslope subsurface flow component through the upper layer of ashes. The short duration of flow diversion depended not only on the contrast of texture between adjoining layers, but also on the initial condition of the pumices, as well as on the applied rainfall intensity, i. In fact, for the given hydraulic properties of the

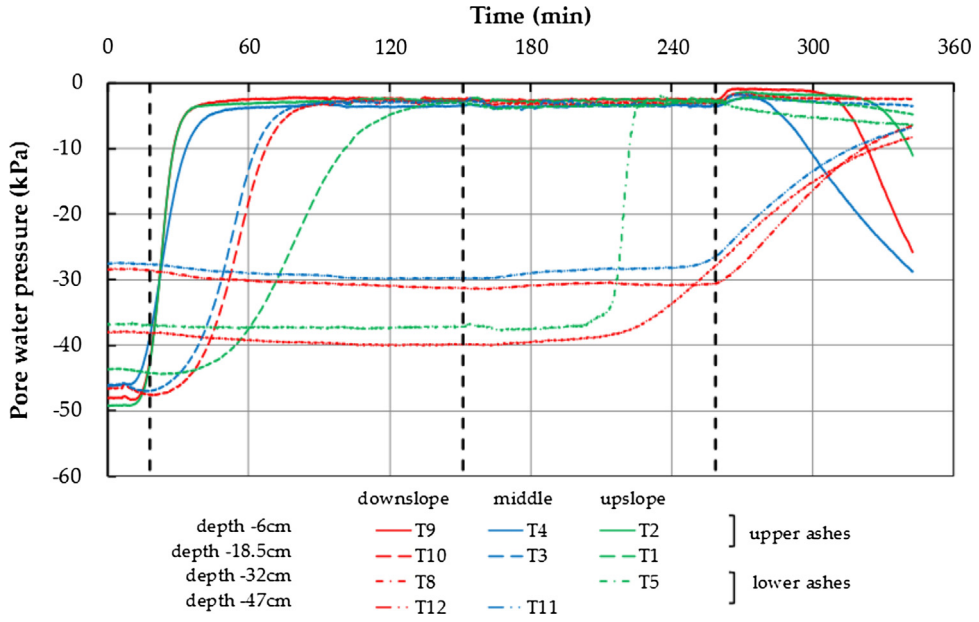

Fig. 7. Water potential measured during and after the infiltration test by the tensiometers placed at various depths along three alignments (i.e. downslope, middle and upslope) within the layered deposit. For the positions of the three verticals see Fig. 5.

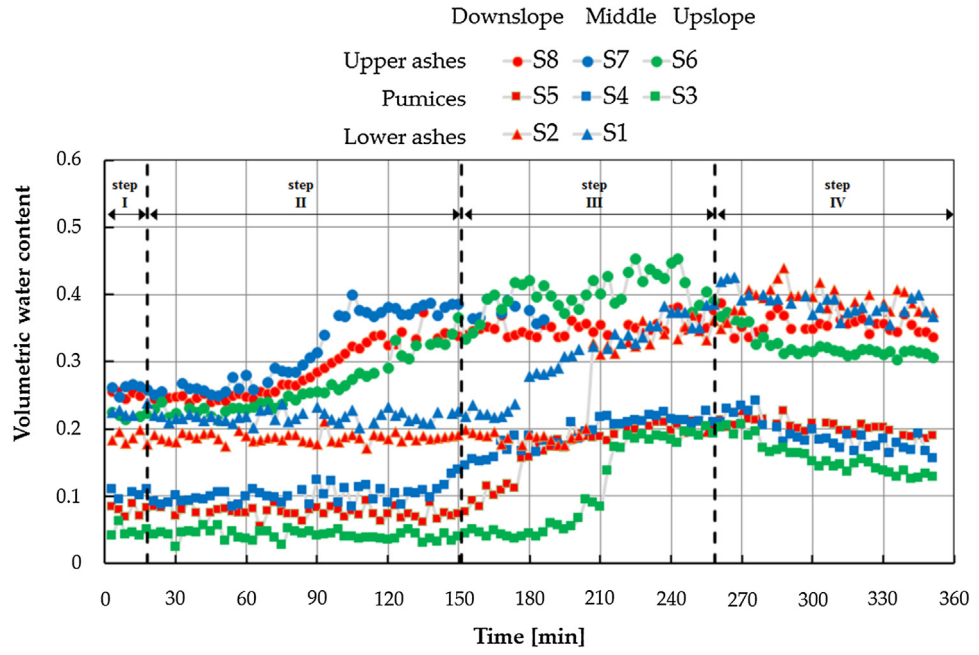

Fig. 8. Soil water content measured during and after the infiltration test by the TDR probes placed at various depths along three alignments (i.e. downslope, middle and upslope) within the layered deposit. For the positions of the three verticals see Fig. 5.

soils, the water potential gradient, required for the progress of the infiltration into the pumices without accumulation of water above the interface, should accommodate the infiltrating flow rate q_n with the existing hydraulic conductivity:

$$q_n = k_p(\cos\alpha + \partial\psi/\partial n) \quad (1)$$

In Eq. (1), n represents the direction orthogonal to the interface, α is the inclination angle of the interface, k_p is the unsaturated hydraulic conductivity of the pumices. The gravity-driven downslope flow q_s along the interface (i.e. neglecting any water potential gradient parallel to it) has the following expression, in which k_a represents the unsaturated hydraulic conductivity of the ashes:

$$q_s = k_a \sin\alpha \quad (2)$$

Owing to the coarse texture of the pumices, in dry conditions and with the high applied rainfall intensity, it is likely $k_p \ll i$. Hence, the establishment of a water potential gradient $\partial\psi/\partial n \gg 1$ is required before the infiltrating water can cross the interface between ashes and pumices. The resulting accumulation of water above the interface causes the increase of the hydraulic conductivity of ashes and, if $k_a \gg k_p$, so that a significant downslope diverted flow q_s may be promoted before infiltrating water crosses the interface (Fig. 11b). Once the gradient in Eq. (1) becomes large enough, the pumices below the interface progressively get wet, their conductivity grows, the hydraulic gradient above the interface reduces, and, when $q_n \cong i\cos\alpha$, the flow through the upper ashes tends to become vertical, and q_s disappears (Fig. 11c). Therefore, the persistence of the diverted flow is strictly

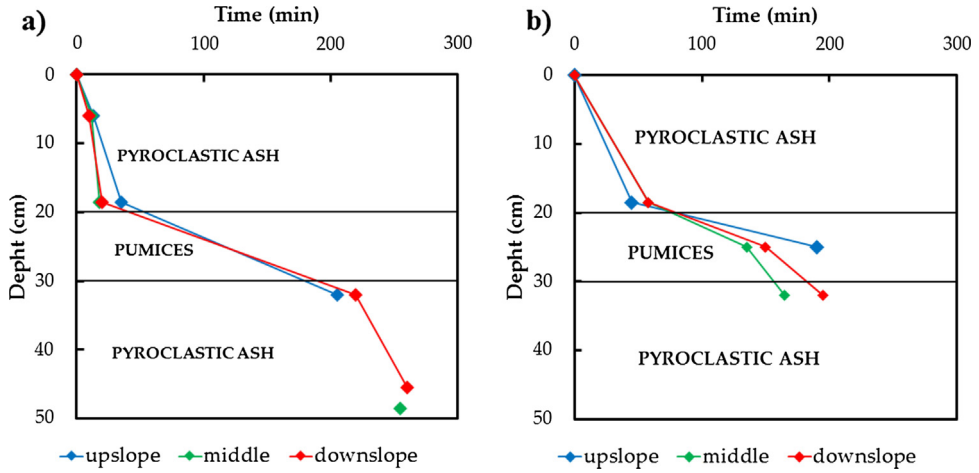

Fig. 9. Arrival times of the wetting front at various depths in the investigated alignments: a) onset of suction variation as detected by tensiometers; b) onset of soil moisture variation as detected by TDR probes.

related to the interplay between the hydraulic properties of the two adjoining soils, the initial dryness of the profile, and the infiltration rate, in turn related to the applied rainfall intensity. In fact, the phenomenon is controlled by how small is k_p at the beginning of the infiltration, how the ratio k_a/k_p across the interface changes in time with varying ψ, and how wet the pumices should become to achieve $k_p \cong i$.

The obtained experimental results indicate that, even starting from quite dry conditions (water pressure between -30 kPa and -40 kPa) and with high applied rainfall intensity, the contrast in the hydraulic properties between the studied ashes and pumices was not enough to promote the formation of downslope diverted flow capable of transferring a significant amount of water towards the foot of the slope. Although rainfall events with high intensity are not rare (e.g. a rain event lasting 18 min with mean intensity of 32 mm/h, like the first phase of the experiment, happens nearly every year), they mostly occur when the soil is already wet. Hence, this result seems to indicate that in real slopes, with layers of volcanoclastic soils like those studied here, infiltration mostly develops either orthogonally to the slope surface (i.e. capillarity-driven, for initially dry soil) or vertically (i.e. gravity-driven, for wet soil).

These findings somehow confirm the results of the simulations, carried out by Mancarella et al. (2012), Guadagno (1991) for a slope with layers of volcaniclastic ashes and pumices resembling those studied here, in which long-lasting capillary barrier and associated downslope flow component, along the interface between the layers, were guaranteed by the very dry initial conditions, and by the extremely different hydraulic characteristic curves assumed for the two soils (Mancarella and Simeone, 2012).

The outflows from the layer of pumices, registered from about 140 min onward, as well as from the lower layer of ashes, starting about 200 min from the beginning of the test, are both too small to be interpreted as the result of downslope flow components through the two lower layers. In fact, even the peaks of about 3–4 l/h, outflowing from the lower layer of ashes, are less than the outflow corresponding to the vertical propagation of the applied rainfall rate of 50 mm/h. Hence, in this phase of the test, most of the water infiltrating in the lower ashes was still stored within the layer, as also indicated by the still growing water content measured by TDR probes S1 and S2 until the end of the

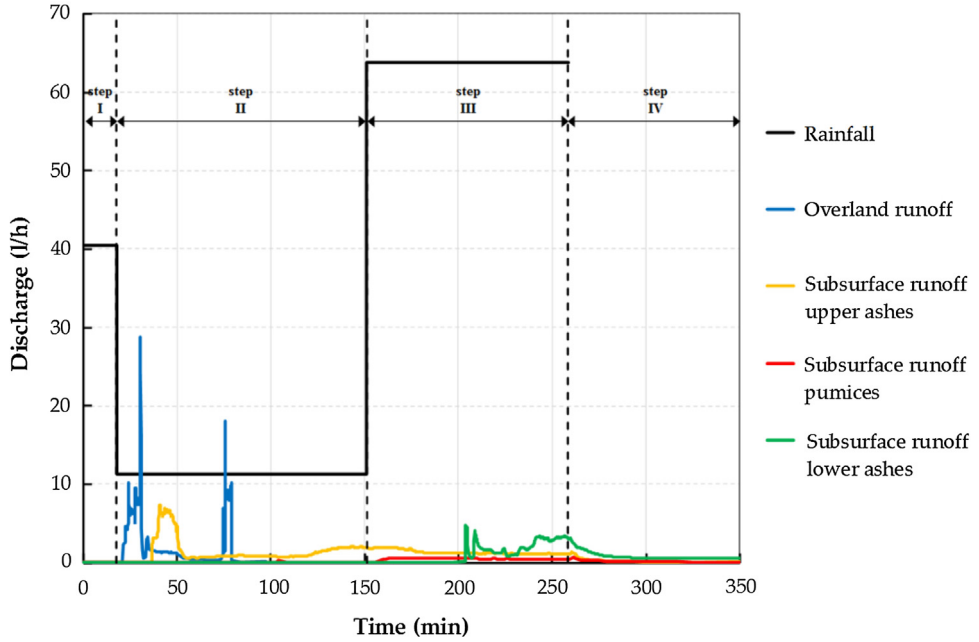

Fig. 10. Discharges measured at the outlet of the gutters, placed on the downslope perforated panel, to collect the overland runoff and the subsurface runoff through the three layers.

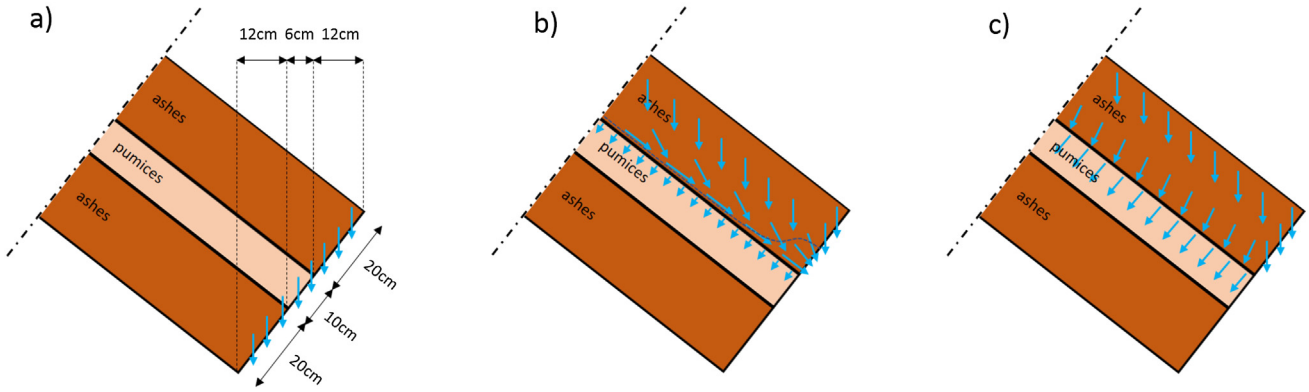

Fig. 11. Sketch of the downslope end of the layered deposit, with indication of the widths of the projections, over a horizontal plane, of the thicknesses of the three layers, with a vertically-directed outflow (a), a partially downslope-directed outflow through the upper layer (b), a partially downslope-directed outflow through the upper layer (b), and the infiltration flow penetrating the pumices (c).

rainfall (Fig. 8).

A further confirmation of the interpretation of the behavior of the layered deposit, during the infiltration test, is offered by plotting the water balance in Fig. 12.

In the graph, the water storage in the soil is estimated, by assuming that the specific volume of water stored within a soil layer could be calculated based on the average of the water contents measured by the TDR probes buried in it, multiplied by the thickness of that layer. In the same graph, the cumulated rainfall and runoff, both overland and subsurface, are also plotted. The overland runoff could be measured only in the first 100 min because soil material, carried by the flow, blocked the outlet of the gutter and made the measured outflow unreliable. After that time, however, the overland runoff could be estimated (accepting a negligible margin of error) as the difference between cumulated rainfall and the sum of soil storage and subsurface runoff.

The estimated trend of the soil storage presents two abrupt jumps, one around 90 min from the beginning of the test, the other after about 200 min. These jumps should be considered artifacts, due to the position of the TDR probes, placed at some distance below the upper interface of each layer and used to estimate their total water storage. So, the increment of water content was detected with some delay, and it was suddenly ascribed to the entire layer, even if water entered gradually. With the progress of the infiltration, the water content distribution within each layer became smoother, and the estimated storage became more reliable. Hence, the plot confirms that, during the first two phases of the test, respectively characterized by rainfall intensity of 32 mm/h and 9 mm/h, overland runoff did not subtract a significant amount of water, as the sum of cumulated subsurface runoff and soil storage after 150 min was practically equal to the cumulated rainfall. Similarly, also during the third phase of the test, with rainfall intensity of 50 mm/h, the overland runoff was initially small. Hence, for nearly four hours, the applied 90 mm rainfall was mostly stored within the deposit, with the sum of overland and subsurface runoff accounting for less than 10 mm.

Only after about 230 min, when the soil storage seemed to reach a nearly stable value, the overland runoff, estimated in this phase as the difference between the other measured terms of the water balance, became the major component of the water balance, subtracting nearly all the 12.5 mm of rainfall applied in the last 15 min before the end of the rainfall.

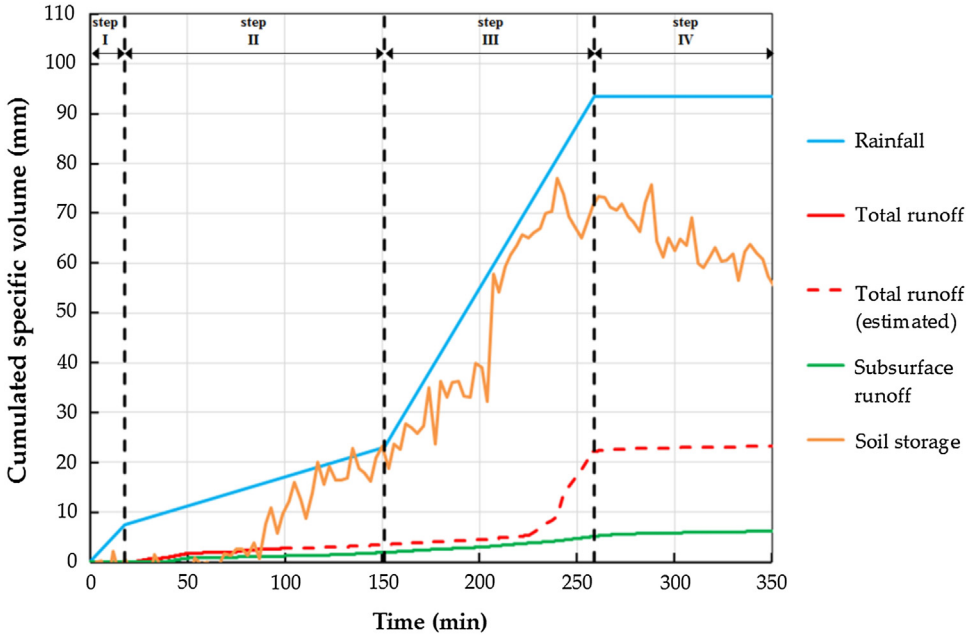

Fig. 12. Water balance in the layered deposit during the infiltration test.

4. Conclusions

The infiltration of rainfall, with variable intensity, into a sloping layered volcanoclastic deposit has been studied by means of physical modeling. Specifically, a three-layered deposit inclined at 38°, with a layer of coarse pumices interbedded between two layers of finer ashes, was instrumented with TDR probes tensiometers, for the measurement of soil water content and suction, and gutters for the collection and measurement of overland and subsurface runoff, from each layer, at the foot of the slope. Starting form a relatively dry condition, with water pressure between −50 kPa and −30 kPa, and water contents between 0.05 and 0.1, in the pumices, and 0.18 and 0.26, in the ashes, the deposit was subjected for more than four hours to a rainfall of variable intensity, starting with 32 mm/h, then reduced to 9 mm/h, and finally increased to 50 mm/h.

The obtained results indicate that the layer of initially dry coarse pumices delayed the advancement of the wetting front, inducing the accumulation of water into the overlying ashes, and the temporary establishment of a downslope-directed subsurface flow, driven by the component of gravity parallel to the slope. This was due to the very small value of the unsaturated conductivity of dry pumices, which required the building up of a high gradient of pressure, to let the water penetrate through them. However, for the considered experimental conditions, the textural difference between the ashes (sandy loam) and pumices (gravel with sand) was not so large to let this condition persist for long time, and after about 10 min, as soon as the infiltration through the pumices started, the subsurface runoff stopped. Afterwards, the infiltration process continued with flow direction always between orthogonal to the slope, when the prevailing gradient was due to capillarity, and vertical, when gravity dominated. The amount of water drained by the subsurface runoff towards the foot of the slope was therefore quite small, compared to the total infiltrated volume. The persistence of the diverted flow for a longer time would be favored by a dryer initial condition and by the application of a higher rainfall intensity.

However, considering that the duration and intensity of the applied rainfall were quite extreme (i.e. more than 90 mm falling in about four hours), the obtained results suggest that, in real slopes, it is very unlikely that the presence of coarse layers of pumices might induce the establishment of significant downslope subsurface drainage, nor the attainment of saturation in the overlying finer layers. The infiltration processes might be only temporarily delayed, but with flow mostly remaining orthogonal to the slope surface. This result indicates that the layers of pumices very unlikely cause the overlying ashes to become so wet to compromise their equilibrium and to trigger landslides along the investigated slopes.

Declaration of Competing Interest

The authors declare that they have no known competing financial interests or personal relationships that could have appeared to influence the work reported in this paper.

Acknowledgments

The authors gratefully acknowledge the financial support provided by the framework of the SILA—PONa3_00341 project An Integrated System of Laboratories for the Environment.

References

Allocca, V., De Vita, P., Manna, F., Nimmo, J.R., 2015. Groundwater recharge assessment at local and episodic scale in a soil mantled perched karst aquifer in southern Italy. J. Hydrol. 529, 843–853.

Aubertin, M., Cifuentes, E., Apithy, S.A., Bussière, B., Molson, J., Chapuis, R.P., 2009. Analyses of water diversion along inclined covers with capillary barrier effects. Can. Geotech. J. 46 (10), 1146–1164.

Basile, A., Mele, G., Terribile, F., 2003. Soil hydraulic behaviour of a selected benchmark soil involved in the landslide of Sarno 1998. Geoderma 117, 331–346.

Baum, R.L., Godt, J.W., Savage, W.Z., 2010. Estimating the timing and location of shallow rainfall-induced landslides using a model for transient, unsaturated infiltration. J. Geophys. Res. 115, F03013.

Bilotta, E., Cascini, L., Foresta, V., Sorbino, G., 2005. Geotechnical characterisation of pyroclastic soils involved in huge flowslides. Geotech. Geol. Eng. 23, 365–402.

Bogaard, T.A., Greco, R., 2016. Landslide hydrology: from hydrology to pore pressure. Wiley Interdiscip. Rev. Water 3, 439–459.

Capparelli, G., Spolverino, G., Greco, R., 2018. Experimental determination of TDR calibration relationship for pyroclastic ashes of Campania (Italy). Sensors 18, 3727. https://doi.org/10.3390/s18113727.

Capparelli, G., Versace, P., 2014. Analysis of landslide triggering conditions in the Sarno area using a physically based model. Hydrol. Earth Syst. Sci. 18, 3225–3237.

Cascini, L., 2004. The flowslides of May 1998 in the Campania region, Italy: the scientific emergency management. Italia Geotech. J. 2, 11–44.

Cascini, L., Cuomo, S., Guida, D., 2008a. Typical source areas of May 1998 flow-like mass movements in the Campania region, Southern Italy. Eng. Geol. 96, 107–125.

Cascini, L., Ferlisi, S., Vitolo, E., 2008b. Individual and societal risk owing to landslides in the Campania region (southern Italy). Georisk: Assess. Manage. Risk Eng. Syst. Geohazards 2 (3), 125–140. https://doi.org/10.1080/17499510802291310.

Cascini, L., Sorbino, G., Cuomo, S., Ferlisi, S., 2014. Seasonal effects of rainfall on the shallow pyroclastic deposits of the Campania region (southern Italy). Landslides 11, 779–792.

Collins, B.D., Znidarcic, D., 2004. Stability analyses of rainfall induced landslides. J. Geotech. Geoenviron. Eng. 130 (4), 362–372.

Comegna, L., Damiano, E., Greco, R., Guida, A., Olivares, L., Picarelli, L., 2016. Field hydrological monitoring of a sloping shallow pyroclastic deposit. Can. Geotech. J. 53 (7), 1125–1137.

Damiano, E., 2018. Effects of layering on triggering mechanisms of rainfall-induced landslides in unsaturated pyroclastic granular soils. Can. Geotech. J online first.

Damiano, E., Olivares, L., 2010. The role of infiltration processes in steep slope stability of pyroclastic granular soils: laboratory and numerical investigation. Nat. Hazards 52 (2), 329–350.

Damiano, E., Olivares, L., Picarelli, L., 2012. Steep-slope monitoring in unsaturated pyroclastic soils. Eng. Geol. 137–138, 1–12.

Damiano, E., Greco, R., Guida, A., Olivares, L., Picarelli, L., 2017. Investigation on rainwater infiltration into layered shallow covers in pyroclastic soils and its effect on slope stability. Eng. Geol. 220, 208–218.

Del Prete, M., Guadagno, F.M., Hawkins, A.B., 1998. Preliminary report on the landslides of 5 May 1998, Campania, southern Italy. Bull. Eng. Geol. Environ. 57, 113–129.

Del Soldato, M., Pazzi, V., Segoni, S., De Vita, P., Tofani, V., Moretti, S., 2018. Spatial modeling of pyroclastic cover deposit thickness (Depth to bedrock) in peri-volcanic area of Campania (southern Italy). Earth Surf. Process. Landf. 43, 1757–1767.

De Vita, P., Agrello, D., Ambrosino, F., 2006. Landslide susceptibility assessment in ashfall pyroclastic deposits surrounding Mount Somma-Vesuvius. Application of geophysical surveys for soil thickness mapping. J. Appl. Geophys. 59, 126–139.

De Vita, P., Fusco, F., Tufano, R., Cusano, D., 2018. Seasonal and event-based hydrological and slope stability modeling of pyroclastic fall deposits covering slopes in Campania (Southern Italy). Water 10, 1140.

De Vita, P., Napolitano, E., Godt, J., Baum, R., 2013. Deterministic estimation of hydrological thresholds for shallow landslide initiation and slope stability models: case study from the Somma-Vesuvius area of southern Italy. Landslides 10, 713–728.

De Vita, P., Piscopo, P., 2002. Influences of hydrological and hydrogeological conditions on debris flows in peri-vesuvian hillslopes. Nat. Hazards Earth. Syst. Sci. 2, 27–35.

Di Martire, D., De Rosa, M., Pesce, V., Santangelo, M.A., Calcaterra, D., 2012. Landslide hazard and land management in high-density urban areas of Campania region, Italy. Nat. Hazards Earth Syst. Sci. 12, 905–926.

Formetta, G., Capparelli, G., 2019. Quantifying the three-dimensional effects of anisotropic soil horizons on hillslope hydrology and stability. J. Hydrol. 570, 329–342.

Formetta, G., Capparelli, G., David, O., Green, T., Rigon, R., 2016. Integration of a three-dimensional process-based hydrological model into the Object Modeling System. Water 8 (1), 12.

Formetta, G., Capparelli, G., Versace, P., 2016. Evaluating performance of simplified physically based models for shallow landslide susceptibility. Hydrol. Earth Syst. Sci. 20, 4585–4603.

Fredlund, D.G., Morgenstern, N.R., 1977. Stress state variables for unsaturated soils. J. Geotech. Eng. Div. 103, 447–466.

Freer, J., McDonnell, J.J., Beven, K.J., Peters, N.E., Burns, D.A., Hooper, R.P., Aulenbach, B., Kendall, C., 2002. The role of bedrock topography on subsurface storm flow. Water Resour. Res. 38, 1269.

Greco, R., Comegna, L., Damiano, E., Guida, A., Olivares, L., Picarelli, L., 2013. Hydrological modelling of a slope covered with shallow pyroclastic deposits from field monitoring data. Hydrol. Earth Syst. Sci. 17, 4001–4013.

Greco, R., Gargano, R., 2015. A novel equation for determining the suction stress of unsaturated soils from the water retention curve based on wetted surface area in pores. Water Resour. Res. 51, 6143–6155.

Guadagno, F.M., 1991. Debris flows in the Campanian volcaniclastic soils. In: Chandler, R.J. (Ed.), Slope Stability Engineering Developments and Applications. Proc. Int. Conf. on Slope Stability, Isle of Wight. 15–18 April 1991, Thoma Telford. pp. 125–130. https://doi.org/10.1680/ssedaa.16606.0021.

Hübner, R., Günther, T., Heller, K., Noell, U., Kleber, A., 2017. Impacts of a capillary barrier on infiltration and subsurface stormflow in layered slope deposits monitored with 3-D ERT and hydrometric measurements. Hydrol. Earth Syst. Sci. 21, 5181–5199.

Jukić, D., Denić-Jukić, V., 2009. Groundwater balance estimation in karst by using a

conceptual rainfall-runoff model. J. Hydrol. 373, 302–315.
Kämpf, M., Holfelder, T., Montenegro, H., 2003. Identification and parameterization of flow processes in artificial in capillary barriers. Water Resour. Res. 39 (10), 1276.
Khire, M.V., Benson, C.H., Bosscher, P.J., 2000. Capillary barriers: design variables and water balance. J. Geotech. Geoenv. Eng. 126, 695–708.
Lanni, C., McDonnell, J.J., Hopp, L., Rigon, R., 2013. Simulated effect of soil depth and bedrock topography on near surface hydrologic response and slope stability. Earth Surf. Proc. Land. 38, 146–159.
Lu, N., Godt, J.W., 2008. Infinite slope stability under steady unsaturated seepage conditions. Water Resour. Res. 44, W11404.
Lu, N., Godt, J.W., Wu, D.T., 2010. A closed-form equation for effective stress in unsaturated soil. Water Resour. Res. 46, W05515.
Lu, N., Kaya, B.S., Godt, J.W., 2011. Direction of unsaturated flow in a homogeneous and isotropic hillslope. Water Resour. Res. 47, W02519.
Mancarella, D., Simeone, V., 2012. Capillary barrier effects in unsaturated layered soils, with special reference to the pyroclastic veneer of the Pizzo d'Alvano, Campania. Italy. Bull. Eng. Geol. Environ. 71, 791–801.
Mancarella, D., Doglioni, A., Simeone, V., 2012. On capillary barrier effects and debris slide triggering in unsaturated soil covers. Eng. Geol. 147–148, 14–27.
Napolitano, E., Fusco, F., Baum, R.L., Godt, J.W., De Vita, P., 2016. Effect of antecedent-hydrological conditions on rainfall triggering of debris flows in ash-fall pyroclastic mantled slopes of Campania (southern Italy). Landslides 13, 967–983.
Olivares, L., Damiano, E., Greco, R., Zeni, L., Picarelli, L., Minardo, A., Guida, A., Bernini, R., 2009. An instrumented flume to investigate the mechanics of rainfall-induced landslides in unsaturated granular soils. Geotech. Test. J. 32 (2), 108–118.
Olivares, L., Damiano, E., Netti, N., de Cristofaro, M., 2019. Geotechnical properties of two pyroclastic deposits involved in catastrophic flowslides for implementation in early warning systems. Geosci. 9 (1), 24.
Rahardjo, H., Aung, K.K., Leong, E.C., Rezaur, R.B., 2004. Characteristics of residual soils in Singapore as formed by weathering. Eng. Geol. 73 (1–2), 157–169.
Rahardjo, H., Santoso, V.A., Leong, E.C., Ng, Y.S., Tam, C.P.H., Satyanaga, A., 2013. Use of recycled crushed concrete and Secudrain in capillary barriers for slope stabilization. Can. Geotech. J. 50 (6), 662–673.
Revellino, P., Guadagno, F.M., Hungr, O., 2008. Morphological methods and dynamic modelling in landslide hazard assessment of the Campania Apennine carbonate slope. Landslides 5, 59–70.
Rolandi, G., Bellucci, F., Heizler, M.T., Belkin, H.E., De Vivo, B., 2003. Tectonic controls on the genesis of ignimbrites from the Campanian Volcanic Zone, southern Italy. Mineral. Petrol. 79, 3–31.
Ross, B., 1990. The diversion capacity of capillary barriers. Water Resour. Res. 26 (10), 2625–2629.
Schneider, P., Pool, S., Strouhal, L., Seibert, J., 2014. True colors – experimental identification of hydrological processes at a hillslope prone to slide. Hydrol. Earth Syst. Sci. 18, 875–892.
Sidle, R.C., Tsuboyama, Y., Noguchi, S., Hosoda, I., Fujieda, M., Shimizu, T., 2000. Stormflow generation in steep forested headwaters: a linked hydrogeomorphic paradigm. Hydrol. Process. 14, 369–385.
Sorbino, G., Nicotera, M.V., 2013. Unsaturated soil mechanics in rainfall-induced flow landslides. Eng. Geol. 165, 105–135.
Soulsby, C., Piegat, K., Seibert, J., Tetzlaff, D., 2011. Catchment-scale estimates of flow path partitioning and water storage based on transit time and runoff modelling. Hydrol. Proc. 25, 3960–3976.
Spolverino, G., Capparelli, G., Versace, P., 2019. An instrumented flume for infiltration process modeling, landslide triggering and propagation. Geosciences 9 (3), 108. https://doi.org/10.3390/geosciences9030108.
Stormont, J.C., Anderson, C.E., 1999. Capillary barrier effect from underlying coarser soil layer. J. Geotech. Geoenv. Eng. 125 (8), 641–648.
Tallon, L.K., O'Kane, M.A., Chapman, D.E., Phillip, M.A., Shurniak, R.E., Strunk, R.L., 2011. Unsaturated sloping layered soil cover system: field investigation. Can. J. Soil Sci. 91, 161–168.
Tami, D., Rahardjo, H., Leong, E.C., Fredlund, D.G., 2004. A physical model for sloping capillary barriers. Geotech. Test. J. 27 (2), 16–26.
Terribile, F., Basile, A., De Mascellis, R., di Gennaro, A., Mele, G., Vingiani, S., 2000. I suoli delle aree di crisi di Quindici e Sarno: proprietà e comportamenti in relazione ai fenomeni franosi del 1998. Quaderni di Geologia Applicata 7, 60–79.
Tromp-van Meerveld, H.J., McDonnell, J.J., 2006. Threshold relations in subsurface stormflow: 2. The fill and spill hypothesis. Water Resour. Res. 42, W02411.
Vanapalli, S.K., Fredlund, D.G., Pufahl, D.E., Clifton, A.W., 1996. Model for the prediction of shear strength with respect to soil suction. Can. Geot. J. 33 (3), 379–392. https://doi.org/10.1139/t96-060.
Vingiani, S., Mele, G., De Mascellis, R., Terribile, F., Basile, A., 2015. Volcanic soils and landslides: a case study of the island of Ischia (southern Italy) and its relationship with other Campania events. Solid Earth 6, 783–797.
Wallace, K.B., 1973. Structural behaviour of residual soils of the continually wet Highlands of Papua New Guinea. Géotechnique 23 (2), 203–218.
Walter, M.T., Kim, J.-S., Steenhuis, T.S., Parlange, J.-Y., Heilig, A., Braddock, R.D., Selker, J.S., Boll, J., 2000. Funneled flow mechanisms in a sloping layered soil: laboratory investigations. Water Resour. Res. 36 (4), 841–849.
Warrick, A.W., Wierenga, P.J., Pan, L., 1997. Downward water flow through sloping layers in the vadose zone: analytical solutions for diversions. J. Hydrol. 192, 321–337.
Wheeler, S.J., Sharma, R.S., Buisson, M.S.R., 2003. Coupling of hydraulic hysteresis and stress–strain behaviour in unsaturated soils. Géotechnique 53, 41–54.
Yang, H., Rahardjo, H., Leong, E.-C., 2006. Behavior of unsaturated layered soil columns during infiltration. J. Hydrol. Eng. 11 (4), 329–337.
Zhan, T.L.T., Li, H., Jia, G.W., Chen, Y.M., Fredlund, D.G., 2014. Physical and numerical study of lateral diversion by three-layer inclined capillary barrier covers under humid climatic conditions. Can. Geotech. J. 51 (12), 1438–1448.
Zegelin, S.J., White, I., Jenkins, D.R., 1989. Improved field probes for soil water content and electrical conductivity measurement using time domain reflectometry. Water Resour. Res. 25, 2367–2376.